JOURNAL OF CATALYSIS **37**, 513–522 (1975)

Surface, Catalytic and Magnetic Properties of Small Iron Particles

III. Nitrogen Induced Surface Reconstruction

J. A. DUMESIC, H. TOPSØE
AND M. BOUDART[1]

Stauffer Laboratories of Chemistry and Chemical Engineering,
Stanford University, Stanford, California 94305

Received October 3, 1974

The turnover number for ammonia synthesis was found to be smaller on very small iron particles than on larger ones, but it could be enhanced by a pretreatment which seemed to bring about a surface reconstruction induced by nitrogen. The same pretreatment decreases the uptake of carbon monoxide by the catalyst and also the anisotropy energy barrier for relaxation of the metallic iron magnetization, as determined by Mössbauer spectroscopy. These new results can be explained by the creation upon pretreatment of the catalyst, of C_7 surface atoms on the small particles, where a C_i atom is one with i nearest neighbors. As the concentration of C_7 atoms is expected to be smaller on very small iron particles than on larger ones, but is enhanced by nitrogen induced surface reconstruction, it is concluded that C_7 iron atoms are more active than others in ammonia synthesis.

INTRODUCTION

Our results (*1*), indicate that the catalytic synthesis of ammonia over iron supported on magnesium oxide is a structure sensitive reaction, i.e., the turnover number depends on particle size. For the small iron particles (ca. 1.5 nm), it was concluded that certain surface sites with a high associated turnover number are created upon reduction of the catalyst, not by pure hydrogen, but by a stoichiometric $H_2:N_2$ mixture. In addition, the hydrogen reduced surface of larger iron particles (>10 nm) was reconstructed by synthesis gas to a far greater extent than that of very small particles.

Since the structure of the iron surface seemed to depend on the nitrogen pressure over that surface, the catalyst was then treated with ammonia to provide a high virtual pressure of nitrogen, and the nitride formed by this treatment was subsequently decomposed in a stoichiometric $H_2:N_2$ mixture. This "ammonia treatment" significantly increased the ammonia synthesis turnover number on the smaller particles, but had no effect on the catalytic activity of the larger particles. In addition, the effect of the ammonia treatment on the small particles could be completely erased by prolonged (ca. 24 hr) reduction of the catalyst at 673 K in pure hydrogen. These results alone, however, do not provide information on the different surface structures. The purpose of the present study, therefore, is to investigate the structure of the iron surface, and its reconstruction by nitrogen, with use of Mössbauer spectroscopy and chemisorption of carbon monoxide.

---

[1] To whom queries should be addressed.

EXPERIMENTAL METHODS

Apparatus

Mössbauer spectra were taken with the spectrometer described elsewhere (*2*). The Mössbauer cell, connecting multipurpose gas handling vacuum system, gases, gas purification, and the apparatus for carbon monoxide chemisorption were the same as those used in part I of this series (*3*).

Catalysts

The samples of iron supported on magnesium oxide used in this study were prepared as already described (*3*). Specifically, 1, 3, 5, and 8% Fe/MgO samples were used, the fraction of the iron as ^{57}Fe being 0.26, 0.32, 0.022, and 0.022, respectively. The dispersion, *D*, of the metal in the reduced 1, 5, and 8% Fe/MgO samples is approximately 0.5, 0.2, and 0.1, respectively (*3*).

The 3% Fe/MgO reduced sample was characterized by magnetic susceptibility and X-ray line-broadening as described elsewhere (*3*). At temperatures greater than 298 K, the data of magnetization, *M*, versus the field divided by the temperature, *H*/*T*, curves could be superimposed on a single curve. This indicates superparamagnetic behavior, and from the low field slope of the curve an average particle size of 5 nm was calculated. The X-ray line-broadening gave an average particle size of 6 nm. Thus, the value of *D* for the 3% Fe/MgO sample is about 0.2.

RESULTS

Mössbauer Spectroscopy

Velocity Modes

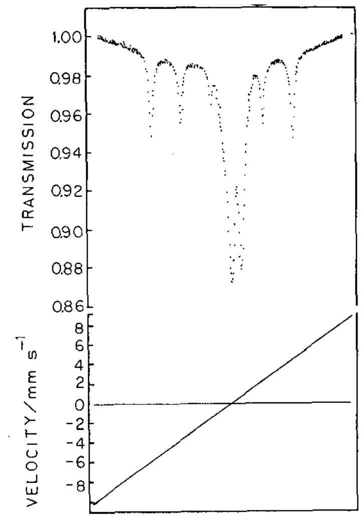

FIG. 1. Mössbauer spectrum (298 K in H_2) of 1% Fe/MgO sample reduced in H_2; constant acceleration mode.

In the previous study (*3*) of the Fe/MgO system, Mössbauer spectra were obtained by scanning the velocity range of ±9 mm s^{-1}, thereby allocating about 20 channels to each metallic iron peak out of the 440 channels used to store γ-ray data. A typical spectrum is shown in Fig. 1, along with the corresponding Doppler velocity mode used to collect the data. Although this spectrum is valuable for simultaneously obtaining information about all the chemical states of iron present in the sample, it is not suited for measuring small changes

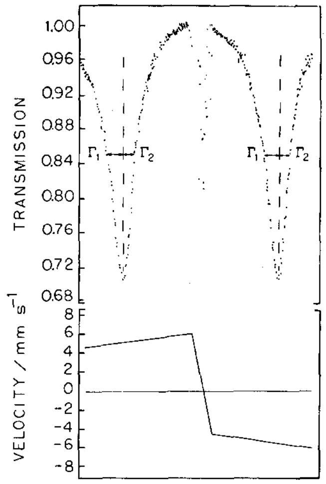

FIG. 2. Mössbauer spectrum (298 K in $H_2:N_2$) of 3% Fe/MgO sample reduced in H_2; velocity offset mode.

(ca. 10%) in the spectral parameters of the metallic iron phase alone. For this reason, the constant acceleration velocity mode was replaced in the present study by the velocity offset mode.

A spectrum is shown in Fig. 2 along with the corresponding velocity offset mode used to collect the data. In this mode, the two outer most metallic iron peaks (see Fig. 1) have been simultaneously scanned, with the allocation of about 150 channels to each peak. The uncertainty in the measurement of peak width at half height is about 3%, and the relative uncertainty in the peak area is approximately 5%, thereby making possible a careful study of the effect of various gaseous treatments.

Collection of Data

The 3% Fe/MgO sample was reduced in flowing Pd-diffused H_2 according to the reduction time schedule outlined elsewhere (*3*). A stoichiometric $H_2:N_2$ mixture was then passed over the sample at 682 K for 24 hr, after which velocity offset spectra were taken at 682, 569, 484, 390, and 298 K in the flowing gas mixture. Following the collection of these spectra, the sample was treated with flowing ammonia at 682 K for 1 hr, and the nitride was decomposed at 682 K in the $H_2:N_2$ mixture for 24 hr. Mössbauer spectra were again collected at the above set of temperatures in the flowing gas mixture. A 24 hr treatment of the sample in flowing Pd-diffused H_2 at 682 K was then performed, followed by the switching from hydrogen to a stoichiometric $H_2:N_2$ mixture as the gas flowing over the sample. Mössbauer spectra were recorded at 682, 570, 484, and 390 K after 24 hr exposure of the sample to the $H_2:N_2$. The data collection cycle was completed by treating the sample with ammonia at 682 K for 1 hr, flowing the $H_2:N_2$ mixture over the catalyst at 682 K for 24 hr, and taking velocity offset Mössbauer spectra in the flowing gas mixture at temperatures of 484 and 390 K.

TABLE 1

MÖSSBAUER SPECTRAL PARAMETERS FOR METALLIC IRON ON 3% Fe/MgO AFTER DIFFERENT PRETREATMENTS

T (K)	Width (mm s^{-1})	Area (mm s^{-1})
After Pd-diffused H_2 reduction; spectrum in $H_2:N_2$		
682	0.40	0.140
569	0.36	0.154
484	0.35	0.170
390	0.37	0.180
298	0.33	0.199
After ammonia treatment; spectrum in $H_2:N_2$		
682	0.38	0.135
570	0.34	0.150
484	0.31	0.158
390	0.32	0.171
298	0.31	0.189
After Pd-diffused H_2 treatment; spectrum in $H_2:N_2$		
682	0.42	0.145
570	0.35	0.152
484	0.35	0.166
390	0.36	0.179
After ammonia treatment; spectrum in $H_2:N_2$		
484	0.31	0.158
390	0.30	0.168

The data are collected in Table 1 and Figs. 3 and 4, the metallic iron peak width having been corrected for "thickness line broadening" (*4*). In the absolute area calculations, corrections for the nonresonant background count rate were made according to the procedure described by Housley *et al.* (*5*), the variations in these corrections not exceeding 1% from spectrum to spectrum.

From Fig. 3, it is apparent that the peak width is quite sensitive to the various gaseous treatments of the sample. Thus, it was also measured in the same way for 1 and 8% Fe/MgO, which were reduced in flowing Pd-diffused H_2 according to the

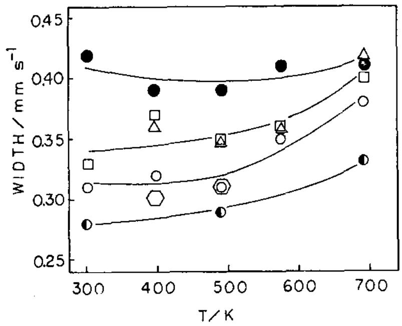

FIG. 3. Metallic iron spectral width in $H_2:N_2$: (●) 1% Fe/MgO after reduction; (□) 3% Fe/MgO after reduction; (○) 3% Fe/MgO after ammonia treatment; (△) 3% Fe/MgO after hydrogen treatment; (○) 3% Fe/MgO after second ammonia treatment; (◐) 8% Fe/MgO after reduction.

prescribed reduction schedule, followed by the exposure to a stoichiometric $H_2:N_2$ mixture for 24 hr at 682 K. The widths so measured, corrected for thickness broadening, are presented in Fig. 3.

Carbon Monoxide Chemisorption

In Fig. 5 are shown the carbon monoxide isotherms at 193 K on 1.0036 g of the dry, reduced 5% Fe/MgO sample. The sample was first reduced in flowing Pd-diffused H_2 according to the prescribed reduction schedule. After evacuation to 10^{-4} Pa for 3 hr at 688 K, the sample was cooled to 193 K, and isotherm A taken. Evacuation to 10^{-3} Pa for 0.5 hr at 193 K followed isotherm A, and then isotherm B was taken. The difference between the two isotherms represents the amount of CO chemisorbed on the metallic iron: 43 ± 1 μmol.

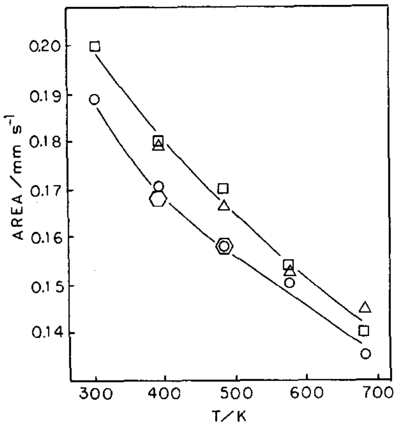

FIG. 4. Metallic iron spectral area in $H_2:N_2$: (□) 3% Fe/MgO after reduction; (○) 3% Fe/MgO after ammonia treatment; (△) 3% Fe/MgO after hydrogen treatment; (○) 3% Fe/MgO after second ammonia treatment.

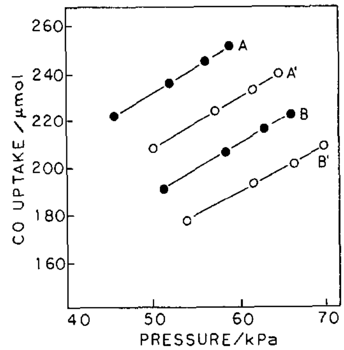

FIG. 5. Carbon monoxide isotherms at 193 K on 5% Fe/MgO sample: (●) before ammonia treatment; (○) after ammonia treatment; (A, A') first isotherms; (B, B') second isotherms.

The sample was then heated to 688 K in flowing hydrogen, and pure ammonia was flowed over the sample for 1 hr at 688 K. Following this treatment, the sample was kept in flowing hydrogen for 1 hr at 688 K, and then evacuated to 10^{-4} Pa for 3 hr at 688 K. Two CO isotherms were then taken at 193 K following the above procedure, and these isotherms are also shown in Fig. 5. The difference between the two isotherms shows that 39 ± 1 μmol of CO was chemisorbed on the metallic iron. If, on the other hand, the first set of isotherms is not followed by an ammonia treatment but by a 12 hr, 688 K hydrogen treatment, no change in the amount of CO chemisorbed on the metallic iron is observed.

DISCUSSION

Mössbauer Spectroscopy

Qualitative Features

For the various gaseous treatments, accompanying changes in the metallic iron Mössbauer spectrum (Fig. 3 and 4) and in the catalytic activity (see Introduction) seem to be related. The ammonia treatment, which increases the turnover number, also decreases the width and area of the metallic iron peak below those values observed after hydrogen reduction. Prolonged hydrogen treatment of the ammonia treated catalyst completely restores the original turnover number as well as the width and area of the metallic iron spectral peak. These effects are totally reversible, as shown by the subsequent ammonia treatment. The interpretation of the changes in the Mössbauer spectra accompanying the various treatments, therefore, may lead to an understanding of the corresponding changes in the surface structure of the iron catalyst.

In another study (*1*), it was shown that the ammonia treatment increases only slightly the total amount of metallic iron present in the 1 and 5% Fe/MgO catalysts, and that this increase is not modified by subsequent hydrogen treatments. Thus, in the present study, the total reversibility in the response of the metallic iron spectral area after cycling the various treatments eliminates changes in the amount of metallic iron as responsible for the reversible changes in spectral area. Instead, changes in this spectral area must reflect changes in the superparamagnetic properties of the metallic iron particles, since all spectra were taken under identical conditions, i.e., a flowing $H_2:N_2$ mixture at a standard set of temperatures. Thus, the changes in the metallic iron peak must be attributed to changes in particle size, size distribution and/or anisotropy energy constant. Again, the reversibility of the changes seems to rule out the alternatives, leaving the anisotropy energy constant as the parameter sensitive to gaseous treatments.

Indeed, in the next paper of this series (*6*) it will be shown that the superparamagnetic properties of the 1 and 3% Fe/MgO samples are dominated by surface effects, i.e., the largest magnetic energy anisotropy is created by the surface. Thus, the different gaseous treatments which change the iron surface structure are expected to change the superparamagnetic properties of the metallic iron spectral component, as experimentally observed. As the anisotropy energy constant, and thus also the relaxation time, is decreased, the magnetically split spectral area must also decrease at a given temperature, since only those iron atoms with a long enough relaxation time will appear magnetically split in the Mössbauer spectrum. The decrease in the metallic iron spectral area upon ammonia treating must, therefore, reflect a decrease in the magnetic anisotropy created by the ammonia reconstructed surface. This explanation, based on the qualitative changes in the Mössbauer spectra, will now be examined in the light of the quantitative spectral changes.

Quantative Features

As a result of the ammonia treatment there is a decrease in the metallic iron spectral area at all of the studied temperatures, but the magnitude of this change decreases as the temperature is increased to 569 or 682 K. As the temperature is increased, the magnetically split metallic iron spectrum becomes more greatly dominated by the larger iron particles of the particle size distribution since the smaller particles have become superparamagnetic. For these larger particles, the smaller surface to volume ratio attenuates the effect of surface anisotropy on the superparamagnetic properties of the particle magnetization, and the effect of surface changes on the Mössbauer spectrum becomes less pronounced. The decrease in the spectral width accompanying the ammonia treatment is also reasonable. The ammonia treatment decreases the surface anisotropy energy barrier, which has the effect of removing the group of small iron particles, $N(r_c)\ \delta r_c$ from the magnetically split spectral peak (*7*), leaving the larger iron particles contributing to the spectral area, where $N(r)$ is the particle size distribution and r_c is the particle size at which the magnetic relaxation frequency is equal to the nuclear Larmor precession frequency. δr_c is a particle size interval bounded at the small size end by r_c, within which the decrease in the anisotropy energy barrier causes a transition from ferromagnetism to superparamagnetism (for the time scale of Mössbauer spectroscopy). Experimentally, in fact, the spectral width decreases as particle size increases (Fig. 3).

Qualitatively, the increase in the metallic iron spectral width at a given temperature accompanying the decrease in the particle size is expected due to the increased contribution of the surface atoms to the spectral peak. A smaller particle will have a shorter relaxation time than a larger particle, and a surface atom may have a smaller magnetic field than a bulk atom. Both of these effects will tend to asymmetrically broaden the metallic iron peaks toward the center of the spectrum as the particle size is decreased. Indeed, there is a significant increase in the peak asymmetry, Γ_1–Γ_2 (Fig. 2), as the particle size is decreased from 6 nm (Γ_1–$\Gamma_2 = 0.00$ at 298 K) to 1.5 nm (Γ_1–$\Gamma_2 = 0.05$ mm s^{-1} at 298 K). In addition, however, a decrease in the particle size is accompanied by a substantial symmetric broadening of the metallic iron Mössbauer peaks. This broadening can be explained by the quadrupole interaction as follows.

Since the electric potential at the surface is less symmetric than in the bulk, the quadrupole interaction is greater for surface atoms than for a bulk atom, as evidenced by Mössbauer spectra in the absence of magnetic interactions (*8*,*9*). However, in the presence of a strong magnetic interaction the quadrupole interaction depends on the angle between the particle magnetization and the principle component of the electric field gradient tensor (*10*). The electric field gradient at a surface atom is determined by the orientation of that surface. On a single iron particle there are many different surface orientations (with respect to a single coordinate system), but there is only one particle magnetization vector (at a given time). Thus, the quadrupole interaction does not give rise to a well-defined "surface peak," but instead to a rather symmetric broadening of the spectral peak. For spherical and hemispherical particles, this quadrupole broadening will be completely symmetric, and as the particle geometry deviates from this symmetry, the quadrupole broadening will become more asymmetric. In another study (*1*) it was shown that the shape of the iron particles supported on magnesium oxide is not very anisotropic, a result which makes the large, symmetric, spectral width of this study for the small iron particles quite reasonable.

The above discussion dealt with the particle size dependence of the spectral width at a given temperature. As the temperature is increased, the peaks will broaden because of superparamagnetic relaxation (*11*). In competition with this process, however, the line width may become more narrow because the width is more greatly dominated by the larger particles as the temperature is increased. This second process will become more important as the particle size is decreased, since the particle size dependence of the width becomes greater as the particle size is decreased. In addition, as the temperature increases and the relaxation time decreases, the quadrupole–magnetic interaction will tend to be averaged to zero on each surface atom. Since this interaction is weaker than the magnetic interaction alone, the former will begin to average to zero before the latter as the temperature is increased. This provides another process for peak narrowing with increasing temperature, this process again becoming more important as the particle size is decreased. Thus, for the 1% Fe/MgO sample, the broadening and narrowing mechanisms appear to cancel giving a spectral width that is fairly insensitive to temperature, while for the 3 and 8% Fe/MgO samples, the broadening process dominates.

It is now clear that the Mössbauer spectrum reflects changes in both the metallic iron particle size and in the surface structure of these particles. Of importance in subsequent discussions is the fact that the ammonia treatment reconstructs the surface to one which provides a smaller surface anisotropy than the original surface.

Chemisorption of Carbon Monoxide

There is a 10% decrease in CO uptake after the ammonia treatment, but no change after a long hydrogen treatment. Since the hydrogen treatment has no effect on the uptake, the small iron particles are stable for long periods of time at 688 K in hydrogen. Similarly, the Mössbauer spectra indicate that sintering of the iron particles does not accompany the ammonia treatment. Thus, the 10% decrease in CO uptake following the ammonia treatment cannot be explained by sintering. Nor can it be explained by a decrease in the fraction of metallic iron since Mössbauer spectra indicate that the ammonia treatment slightly increases the amount of metallic iron present in the sample. The ammonia treatment, therefore, appears to change the structure of the surface such that the reconstructed surface chemisorbs less carbon monoxide.

The strong bond between carbon monoxide and metallic iron suggests that the chemisorption at low temperatures proceeds to full monolayer coverage, and arguments based on steric considerations in a monolayer have been invoked to account for differences in the carbon monoxide uptake on different crystallographic planes (*12,13*). As a working hypothesis, Brunauer and Emmett (*12*) have assumed that one CO molecule chemisorbs on each surface atom, and that atoms with incomplete coordination but below the surface will not chemisorb a CO molecule. In addition, the most closely packed plane, the (110) plane, was assumed to chemisorb one CO molecule for every two surface atoms due to steric effects. This model for CO chemisorption corresponds to the chemisorption of one CO molecule for every two surface exposed atoms, and this was the assumption made in the determination of the metallic iron particle size from chemisorption measurements (*3*). Westrik and Zwietering (*13*), on the other hand, postulated that one CO molecule would chemisorb on two surface atoms for the (100) plane and three surface atoms for the (110) plane. Due to the lack of agreement between the above two models, the nature of the CO stoichiometry on different crystallographic planes must be discussed further.

It seems reasonable to treat a CO molecule as a cylindrically (or dumbell) shaped molecule, and using this shape the diameter of the cylinder is equal to 0.35 nm (*14*). In order for the model of Brunauer and Emmett to be correct, the size of the CO molecule should lie in the interval from 0.25 to 0.29 nm (the lattice parameter of bcc iron). Clearly, however, such steric arguments cannot be made so rigid, and if a 4% overlap between neighboring CO molecules is allowed, then the 0.35 nm molecular size is compatible with the model of Brunauer and Emmett. The model of Brunauer and Emmett is also in accord with some recent experimental studies of CO chemisorption on single crystal transition metal surfaces. The results of Park and Farnsworth (*15*), although tentative, indicated CO:metal stoichiometries of 1:1 and 1:2 on the nickel (110) and (100) planes, respectively (fcc with $a_0 = 0.352$ nm). The nickel atom densities on the (110) and (100) planes are 1.1×10^{15} and 1.6×10^{15} cm^{-2}, respectively, making these planes analogous to the iron (100) and (110) planes with iron densities of 1.2×10^{15} and 1.7×10^{15} cm^{-2}, respectively. Thus, the assignment of CO:metal stoichiometries of 1:1 and 1:2 on the (100) and (110) planes of iron according to the Brunauer and Emmett model is in agreement with the CO chemisorption results on nickel. In addition, a statement that can be made with some confidence is that CO adsorption coverages of 1.1×10^{15} cm^{-2} on nickel surfaces are quite reasonable (*16*), favoring the model of Brunauer and Emmett over that of Westrik and Zwietering.

The test of the Brunauer and Emmett model is even more direct in the case of CO chemisorption on chromium (bcc with $a_0 = 0.288$ nm). Hague and Farnsworth (*17*) observed a 1:1 CO:metal stoichiometry on the (100) plane of chromium, and in view of the similarity in the chromium and iron structures and lattice parameters, this result is in nice agreement with the prediction of the Brunauer and Emmett model. By no means is it suggested that the details of the chemisorbed state are the same for CO chemisorption on iron, nickel and chromium. However, arguments based on steric considerations will be similar in all three cases, thereby allowing the validity of the Brunauer and Emmett model to be tested.

A thorough discussion of steric considerations in CO chemisorption on metals has been given by Brennan and Hayes (*18*), thereby providing additional support to the Brunauer and Emmett model. The potential energy of interaction between a pair of neighboring adsorbed CO molecules on a surface was chosen following the work of Mason and Rice (*19*), and was used to calculate the CO interaction energies for various CO:metal surface stoichiometries. Indeed, a CO:metal = 1:2 surface stoichiometry for the (110) plane of iron was shown to be quite reasonable, although a 1:1 stoichiometry on the (100) plane involved an interaction energy per adsorbed CO molecule that is approximately equal to the heat of CO adsorption on iron at zero coverage (ca. 160 kJ mol^{-1}). Thus, while the CO:metal surface stoichiometry on the (100) plane of iron may not be strictly 1:1, an average stoichiometry which approaches this value is expected. Brennan and Hayes also considered the (211) plane of iron, and the surface stoichiometry thereby predicted is in complete agreement with the model of Brunauer and Emmett.

The Brunauer and Emmett model as stated above applies to the (100), (111), (110), and (211) planes. For the small iron particles used in this study, however, many high index planes are undoubtedly exposed at the surface. Indeed, characterization of the surface by specifying the many planes present seems to be quite awkward for these small particles. It seems to be much more natural to speak of the concentration of various surface sites when characterizing the catalytic surface, and this is the approach to be used in subsequent discussions. The model of Brunauer and Emmett must now be recast in terms of surface sites rather than surface planes.

Because the size of a CO molecule is larger than that of an iron atom, if a CO molecule chemisorbs on a surface atom with nearest neighbors in the surface, then these nearest neighbors will be sterically blocked from chemisorbing any other CO molecules. The steric blocking of surface atoms that are not nearest neighbors to the chemisorbed surface atom is ruled out by the Brunauer and Emmett model. Also, it is to be remembered that sites below the surface cannot chemisorb CO molecules. These general statements will now be applied to the C_4, C_5, C_6, and C_7 sites (C_i represents a surface atom with i nearest neighbor iron atoms). For convenience, these sites are sketched in Fig. 6.

The C_4 site has no nearest neighbors in the surface. Thus, if a CO molecule chemisorbs on a C_4 site, it blocks that particu-

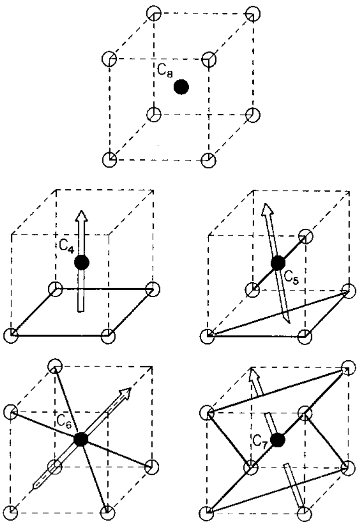

FIG. 6. Surface atoms on bcc structures.

lar site, and four other sites that are not in the surface. However, these four sites can never chemisorb CO molecules; therefore, the blocking of these sites does not impair the ability of the surface to chemisorb CO. The C_5 and C_6 sites have two and four nearest neighbors in the surface, and the steric blocking of these potential CO chemisorbers does indeed decrease the amount of CO uptake for these sites compared to the C_4 site. The geometry of the C_7 site is such that it cannot chemisorb a CO molecule, and hence it has the poorest CO chemisorption ability of any of the other sites.

It can now be said that the following sites are arranged, from left to right, in the order of decreasing CO uptake potential:

$$C_4, C_5, C_6, C_7.$$

It should be noted that the major assumption that has been made in arriving at this sequence of sites is that a CO molecule does not sterically block surface atoms that are not nearest neighbors of the chemisorbed site. This is essentially the Brunauer and Emmett model, which has been shown to be quite reasonable. Since the ammonia treatment decreases the CO chemisorption uptake, it can now be said to reconstruct the surface in such a way that new sites are formed in the following direction:

$$\xrightarrow[\text{ammonia treatment}]{C_4,\ C_5,\ C_6,\ C_7} .$$

CONCLUSION

In the discussion of the Mössbauer spectra, it was shown that the ammonia treatment reconstructs the iron surface in such a manner as to decrease the surface anisotropy. The latter is associated with surface structure as expressed by the nature of atoms denoted by their coordination number. Néel's phenomenological theory of surface anisotropy (*20*) can be used to show (*6*) that the following sites are arranged from left to right in the order of decreasing surface anisotropy:

$$C_6, C_5 \text{ or } C_7, C_4.$$

The effect of the ammonia treatment, therefore, must be a net conversion of surface sites from those on the left to those further toward the right. That is, the effect of the ammonia treatment is to move from left to right on the below sequence of sites:

$$\xrightarrow[\text{ammonia treatment}]{C_6,\ C_5 \text{ or } C_7,\ C_4} .$$

This result, combined with the sequence of sites deduced from carbon monoxide chemisorption, leads to the conclusion that C_7 sites are created by the ammonia treatment. This conclusion is supported by results of other studies.

Brill *et al.* (*21*) found that the (111) plane of iron is preferentially formed upon exposure of the (110) and (100) planes of iron to nitrogen at 673 K. Since the (111) plane of a bcc metal, such as iron, has a high concentration of C_7 atoms (Fig. 7), the present results agree with those of Brill *et al.* Besides, the conclusion that C_7 atoms on iron are particularly active in ammonia synthesis agrees with the find-

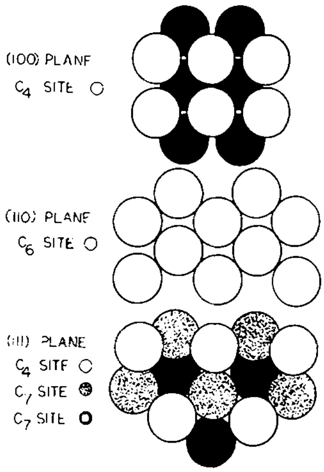

FIG. 7. Low index bcc surface planes and associated surface atoms.

ings of Brill and Kurzidim (*22*) concerning an increase in the rate of ammonia synthesis when an iron surface was pretreated in such a way as to favor the formation of C_7 sites. Finally, McAllister and Hansen (*23*) have reported a rate of ammonia decomposition more than 10 times higher on the (111) than on the (100) and (110) faces of single crystals of tungsten, another bcc metal.

What remains to be done is to explain why C_7 sites are more active in ammonia synthesis or decomposition than other sites on bcc metals. For this, further work is required, with a detailed knowledge of the mechanism of ammonia synthesis at the molecular level.

ACKNOWLEDGMENT

This work was supported by NSF Grant No. GK 17451X. One of us (J.A.D) received support from a NSF Fellowship. Stimulating discussions with Professor Emmett during the early stages of this work are gratefully acknowledged.

REFERENCES

1. Dumesic, J. A., Topsøe, H., Khammouma, S., and Boudart, M., *J. Catal.* **37**, 503 (1975).
2. Topsøe, H., Dumesic, J. A., and Boudart, M., *J. Catal.* **28**, 477 (1973).
3. Boudart, M., Delbouille, A., Dumesic, J. A., Khammouma, S., and Topsøe, H., *J. Catal.* **37**, 486 (1975).
4. Frauenfelder, H., Nagle, D. E., Taylor, R. D., Cochran, D. R. F., and Visscher, W. M., *Phys. Rev.* **126**, 1065 (1962).
5. Housley, R., Erickson, N. E., and Dash, J. D., *Nucl. Instrum. Methods* **27**, 29 (1964).
6. Dumesic, J. A., Topsøe, H., and Boudart, M., *Surface Sci.*, submitted (part IV of this series).
7. Kündig, W., Bömmel, H., Constabaris, G., and Lindquist, R. H., *Phys. Rev.* **142**, 327 (1966).
8. Gager, H. M., Hobson, M. C., and Lefelhocz, J. F., *Chem. Phys. Lett.* **15**, 124 (1972).
9. Bartholomew, C. H., and Boudart, M., *J. Catal.* **29**, 278 (1973).
10. Greenwood, N. N., and Gibb, T. C., "Mössbauer Spectroscopy," p. 63. Chapman and Hall, London, 1971.
11. McNab, T. K., PhD dissertation, Univ. of Western Australia, 1968.
12. Brunauer, S., and Emmett, P. H., *J. Amer. Chem. Soc.* **62**, 1732 (1940).
13. Westrik, R., and Zwietering, P., *Proc. Kon. Ned. Akad. Wetensch. Ser. B* **56**, 492 (1953).
14. Wyckoff, R. W. G., "Crystal Structures," p. 185. Wiley (Interscience), New York, 1965.
15. Park, R. L., and Farnsworth, H. E., *J. Chem. Phys.* **43**, 2351 (1965).
16. Taylor, T. N., and Estrup, P. J., *J. Vac. Sci. Technol.* **10**, 26 (1973).
17. Hague, C. A., and Farnsworth, H. E., *Surface Sci.* **1**, 378 (1964).
18. Brennan, D., and Hayes, F. H., *Phil. Trans. Roy. Soc., Ser. A* **258**, 347 (1965).
19. Mason, E. A., and Rice, W. E., *J. Chem. Phys.* **22**, 843 (1954).
20. Néel, L., *J. Phys. Radium* **15**, 225 (1954).
21. Brill, R., Richter, E. L., and Ruch, E., *Angew. Chem. Int. Ed. Engl.* **6**, 882 (1967).
22. Brill, R., and Kurzidim, J., *Colloq. Int. Cent. Nat. Rech. Sci.* **187**, 99 (1969).
23. McAllister, J., and Hansen, R. S., *J. Chem. Phys.* **59**, 414 (1973).